Clinical Cancer Research

Characterization of the Immune Microenvironment in Hepatocellular Carcinoma

Mark Yarchoan[1], Dongmei Xing[1], Lan Luan[2], Haiying Xu[1], Rajni B. Sharma[1], Aleksandra Popovic[1], Timothy M. Pawlik[3], Amy K. Kim[1], Qingfeng Zhu[1], Elizabeth M. Jaffee[1], Janis M. Taube[1], and Robert A. Anders[1]

Abstract

Purpose: Hepatocellular carcinoma (HCC) often arises in the setting of chronic liver inflammation and may be responsive to novel immunotherapies.

Experimental Design: To characterize the immune microenvironment in HCC, IHC staining was performed for CD8-positive T lymphocytes, PD-1–positive, and LAG-3–positive lymphocytes, CD163-positive macrophages, and PD-L1 expression in tumor and liver background from 29 cases of resected HCC.

Results: Expression of CD8 was reduced in tumor, and expression of CD163 was reduced at the tumor interface. Positive clusters of PD-L1 expression were identified in 24 of 29 cases (83%), and positive expression of LAG-3 on tumor-infiltrating lymphocytes was identified in 19 of 29 cases (65%). The expression of both PD-L1 and LAG-3 was increased in tumor relative to liver background. No association between viral status or other clinicopathologic features and expression of any of the IHC markers investigated was noted.

Conclusions: LAG-3 and PD-L1, two inhibitory molecules implicated in CD8 T-cell tolerance, are increased in most HCC tumors, providing a basis for investigating combinatorial checkpoint blockade with a LAG-3 and PD-L1 inhibitor in HCC. *Clin Cancer Res; 23(23); 7333–9. ©2017 AACR.*

Introduction

Hepatocellular carcinoma (HCC) is an aggressive malignancy that typically develops in the setting of chronic liver disease or cirrhosis. HCC is the second leading cause of cancer-related death in the world (1). The leading risk factor for HCC is cirrhosis arising from viral hepatitis, alcoholic liver disease, and nonalcoholic fatty liver disease (for review, ref. 2). Early-stage HCC can often be treated with potentially curative partial resection or liver transplantation or with locoregional procedures. However, for patients with advanced disease, current systemic treatment options provide only limited therapeutic benefit for a subset of patients, and novel therapeutic options are needed.

Immune checkpoint inhibitors targeting programmed death 1 (PD-1) or its ligand, PD-L1, have demonstrated remarkable clinical activity across a number of different tumor types. In HCC, preliminary signs of activity were observed in the initial clinical trials of these agents, and multiple larger studies are ongoing (3–5). Initial signs of clinical activity have also been observed with therapies targeting another checkpoint pathway, CTL-associated protein 4 (CTLA4), in HCC (6). Responses with these immunotherapy agents have been observed in viral infected and uninfected patients (3). Although larger confirmatory studies are required, these preliminary clinical findings suggest that the immune checkpoint inhibitors may be important in the future management of HCC.

Recent studies have begun to define the immune microenvironment in HCC. PD-L1 expression is increased in some HCC tumors, and PD-L1 expression in this tumor type has been correlated with aggressive disease and poorer survival in recent series (7–10). In addition, increased plasma concentration of the soluble form of CD163 (sCD163), a marker of alternatively activated macrophages (M2), has been observed in HCC and may be associated with poor survival (11, 12) indicating that M2 macrophages may be a potential target for HCC immunotherapy. However, the clinical significance of this association has been disputed in another series because sCD163 may be reflective of active hepatitis rather than meaningful tumor characteristics (13).

Less is known about other checkpoint signals within HCC tumors. However, a number of other inhibitory signals are often coexpressed with PD-1 on effector T cells that downregulate their activity in tumors. For example, the lymphocyte activation gene-3 (LAG-3) is commonly expressed on the surface of T cells and is thought to regulate and inhibit T-cell activation. As with other immune checkpoints, LAG-3 has been implicated in tumor escape and has recently emerged as a potential target for immune modulation in cancer therapy (14). However, to our knowledge, the expression of LAG-3 has not previously been assessed in HCC. Here, we characterize the expression of CD8, CD163, PD-1, PD-L1, and LAG-3 in HCC. Our findings provide new insights into the immunomodulatory signals within the HCC tumor microenvironment that regulate effector T-cell responses.

[1]The Bloomberg-Kimmel Institute for Cancer Immunotherapy at Johns Hopkins, Baltimore, Maryland. [2]Department of Pathology, Central Hospital affiliated with Shenyang Medical College, Shenyang, Liaoning Province, China. [3]Ohio State University Wexner Medical Center, Columbus, Ohio.

Note: M. Yarchoan and D. Xing contributed equally to the article.

Corresponding Author: Robert A. Anders, Johns Hopkins Medical Institutions, 401 North Wolfe Street, Baltimore, MD 21287. Phone: 410-955-3511; Fax: 410-614-0671; E-mail: rander54@jhmi.edu

doi: 10.1158/1078-0432.CCR-17-0950

Translational Relevance

Tumors frequently co-opt the expression of multiple inhibitory immune signals (immune checkpoints) to reduce antitumor immunity. Immune checkpoint inhibitors are designed to block these inhibitory leading to increased activity of T cells specific for tumor antigens. Immune checkpoint inhibitors targeting programmed death 1 (PD-1) have clinical activity in many tumor types, including hepatocellular carcinoma (HCC). We have characterized the immune microenvironment in HCC and find that lymphocyte activation gene-3 (LAG-3) is increased in HCC tumors relative to liver background. Multiple LAG-3 inhibitors are in early stages of clinical development, and our results provide a basis for investigating combinatorial checkpoint blockade with an LAG-3 and PD-1 inhibitor in HCC.

Materials and Methods

HCC specimens and IHC staining

This research was performed in accordance with the Declaration of Helsinki, and the study protocol was approved by the Institutional Review Board (IRB) at Johns Hopkins. A total of 29 cases of untreated, primary HCC resected at Johns Hopkins Hospital from 2011 to 2014 were identified. Clinical information pertaining to these cases was extracted from the Johns Hopkins Hospital electronic medical record. The diagnosis was confirmed by two pathologists (R.A. Anders and D. Xing) and through review of hematoxylin and eosin (H&E) slides of each case.

Staining for PD-L1 (15) and PD-1 (16) was performed as previously described. Immunohistochemistry (IHC) staining for LAG3, CD8, and CD163 were performed according to standardized institutional protocols. Briefly, one representative formalin-fixed paraffin-embedded (FFPE) block from each tumor specimen was selected with tumor and background liver tissue on the same block. Consecutive 5-μm-thick sections were cut from each block and mounted on glass slides. After deparaffinization and rehydration, antigen retrieval, antibody staining, and detection were performed as shown in Table 1. All slides were counterstained with hematoxylin, dehydrated, and cover slipped.

Quantitation of CD8, PD-1, and CD163

Slides were scanned at 20× objective equivalent (0.49 μm/pixel) using an Aperio Scanscope. A trained gastrointestinal pathologist determined the tumor/background liver interface. The prevalence of positive stained cells for each marker was recorded in tumor, interface tumor side, interface background liver side, and background liver compartments. Image analysis (HALO Indica Labs) was used to determine the density (# of cells/surface area analyzed) of CD8 and PD-1–expressing lymphocytes and CD163-expressing cells within each of the four tissue compartments as described previously (17, 18).

Quantification of PD-L1 and LAG-3

Scoring of PD-L1 expression on tumor and LAG-3 expression on infiltrating lymphocytes was performed manually by two separate pathologists (R.A. Anders and D. Xing), working independently, who were blinded to the demographic features of the case while performing the scoring. The scoring of the two pathologists was subsequently averaged into a combined final score. For PD-L1 expression, the number of cell clusters (defined as more than five adjacent cells staining with PD-L1 in a cell surface/membranous pattern) was counted in tumor and background liver. Clusters of hepatocytes or infiltrating immune cells expressing PD-L1 were both included in this count. The density of PD-L1 expression was subsequently determined by dividing the number of cell clusters by the surface area analyzed to obtain a final cluster density score. The percentage of LAG-3–positive lymphocytes was determined by dividing the number of LAG-3–positive lymphocytes by the total number of lymphocytes counted across five low-power fields in tumor and liver background sections.

Statistical analysis

The mean expression of CD8, CD163, PD-1, PD-L1, and LAG-3 in the various tissue compartments (background liver, interface background liver, interface tumor side, and tumor) was compared using Wilcoxon signed-rank tests. The relationship between patient or tumor characteristics and the expression of these IHC markers in tumor was explored using Wilcoxon rank-sum tests and correlations with appropriate transformations. Statistical analyses were performed with GraphPad Prism 7 (GraphPad Software, Inc.) and confirmed in JMP 11 (SAS Institute Inc.). All statistical tests were two-sided, and *P* values of less than 0.05 were considered to be statistically significant for all analyses.

Results

It is now clear that tumors attract many different immune subsets into their microenvironment that can have both immunosuppressive and effector functions. Whether this immune infiltration results in immune suppression or tumor rejection is determined both by the summation of the functional capabilities of each subset and the location of these subsets relative to tumor cells. Some untreated tumors will have dense immune infiltration in the normal or reactive tissue surrounding the tumor but few

Table 1. IHC staining procedures for CD8, CD163, PD-1, PD-L1, and LAG-3

Antibody	Clone	Source	Antigen retrieval	Primary Ab incubation	Instrument/detection
CD8	C8/144B	Cell Marque	EDTA buffer, pH 9.0	40	Biotin-conjugated second antibody, visualized with a DAB chromogen (Ventana Ultra)
CD163	10D6	Leica	Citrate buffer, pH 6.0	30	HRP-conjugated polymer, visualized with a DAB chromogen (Leica-Bond III)
PD-1	NAT105	Abcam	Citrate buffer, pH 6.0	Overnight, 4°C	Tyramide signal amplification (TSA) system (PerkinElmer)
PD-L1	SP142	Spring bioscience	Citrate buffer, pH 6.0	Overnight, 4°C	Tyramide signal amplification (TSA) system (PerkinElmer)
LAG-3	17B4	Lifespan bioscience	Citrate buffer, pH 6.0	Overnight, 4°C	Biotin-conjugated second antibody (BD Pharmingen 553441), amplified by TSA Plus Biotin Kit (PerkinElmer NEL749B001KT), detected with a peroxidase-conjugated streptavidin (Dako P0397) visualized by DAB (Sigma D4293)

immune cells infiltrating the tumor. These infiltrate characteristics can determine which immune modulating agents may be effective in altering this inflammatory response to one that can infiltrate and eradicate tumor. We recently developed an IHC approach that analyzes immune targets on serially cut slides and uses both an image analysis approach and a manual approach to quantitate the density of each target on different immune cell subtypes in different areas of the tumor microenvironment. This approach was applied for the first time to 29 cases of untreated HCC.

The characteristics of the study group are displayed in Table 2. The median age of subjects at the time of the resection was 62 and the majority of subjects (83%) had background cirrhosis. Among the patients included in this cohort, 14 patients had undergone a liver transplantation, and 15 patients had undergone a curative-intent surgical resection of HCC. At the time of analysis, five patients had relapsed disease, four subjects had died, and two subjects were lost to follow-up.

Figure 1 demonstrates examples of IHC staining for PD-L1 and CD163. The mean density of CD8-positive infiltrating T lymphocytes in background liver, tumor interface, and tumor is shown in Fig. 2. The mean density of CD8-positive T lymphocytes was significantly lower in tumor than in the background liver (14.3 cells/mm^2 vs. 43.0 cells/mm^2, $P < 0.001$). At the tumor interface, the mean density of CD8-positive lymphocytes was higher on the nontumor (or "liver") side than the tumor side of the interface (46.5 cells/mm^2 vs. 29.3 cells/mm^2, $P < 0.01$), and the density of lymphocytes was similar on the nontumor side of the interface compared with the background liver.

A similar density of CD163-positive macrophages cells was observed in the background liver and tumor sections. However, a lower density of CD163-positive cells was observed at the tumor interface. The mean density of CD163-positive cells was 73.5 cells/mm^2 on the interface liver (or nontumor) side and 71.2 cells/mm^2 on the interface tumor side, which was significantly lower than the background liver (93.4 cells/mm^2; $P < 0.01$ and $P < 0.05$, respectively). The density of PD-1–positive cell staining was similar in the background liver and tumor interface subsections. However, the mean density of PD-1–positive cells was significantly lower in the tumor than in the background liver (4.4 cells/mm^2 vs. 9.8 cells/mm^2, $P < 0.01$).

The mean expression of PD-L1–positive clusters was higher in tumor than liver background (9.8 vs. 4.4 clusters per mm^2, $P < 0.001$). Of the 29 samples analyzed, 24 tumors (83%) had positive PD-L1 expression using a cut-off value of greater than one positive cluster per mm^2. By this same criterion, two of 29 (7%) of liver background samples had positive PD-L1 expression. One was a patient with a history of HBV cirrhosis, and one was a patient with a history of NASH without discernable cirrhosis.

Elevated LAG-3 expression was observed on tumor-infiltrating lymphocytes from multiple patients. Across all samples analyzed, the mean percentage of tumor-infiltrating lymphocytes staining positive for LAG-3 was 13%, which was significantly higher than the 3% of lymphocytes that stained for this marker in the liver background ($P < 0.001$). Using a positive cut-off value of 1%, 19 of 29 of samples (65%) had positive LAG-3 staining of lymphocytes in tumor, whereas 10 of 29 of samples (34%) had positive LAG-3 staining of lymphocytes in liver background. Using a more restrictive cut-off value of 5%, 15 of 29 of samples (52%) had positive LAG-3 staining of lymphocytes in tumor, whereas four of 29 samples (14%) had positive LAG-3 staining of lymphocytes in liver background.

Table 2. Characteristics of the study subjects

Patient characteristics	
Age, y	
Median	62
Range	17–80
Sex, number (%)	
Male	22 (76%)
Female	7 (24%)
Pathology	
Poorly diff	2 (7%)
Moderately diff	20 (69%)
Well diff	7 (24%)
Cirrhosis	
Yes	24 (83%)
No	5 (17%)
Disease stage (T, N)	
T1, N0	5 (17%)
T1, NX	10 (34%)
T2, N0	6 (21%)
T2, NX	4 (14%)
T3, N0	1 (3%)
T3, NX	3 (10%)
AFP	
Median	15.5
Range	1.8–836
Vascular invasion	
Present	8 (28%)
Absent	20 (69%)
Indeterminate	1 (3%)
HCC group	
Viral infected	15 (52%)
HCV	14 (48%)
HBV	1 (3%)
Uninfected	14 (48%)
ASH	5 (17%)
NASH	9 (31%)

Abbreviations: ASH, alcoholic steatohepatitis; NASH, nonalcoholic setatohepatitis.

Many patients with positive LAG-3 staining in tumor-infiltrating lymphocytes also had positive PD-L1 staining in tumor, but there were also several cases with elevated LAG-3 staining in tumor-infiltrating lymphocytes that did not have detectable PD-L1 staining. Across the entire study cohort using a cut-off value of 1%, 17 patients (58%) had both positive LAG-3 and PD-L1 staining in tumor, whereas six patients (21%) had positive PD-L1 staining only, and two patients (7%) had positive LAG-3 staining only. Four patients (14%) had negative PD-L1 and LAG-3 staining. There was no relationship between LAG-3 staining in tumor-infiltrating lymphocytes and the density of PD-1 or CD8 expression in tumor.

As indicated in Table 2, 15 of 29 (52%) of patients from these derived pathology cases were virally infected with HCV or HBV, whereas the remaining cases were uninfected. We investigated the relationship between the presence of viral hepatitis and the density of staining of the various IHC markers in tumor tissue. The mean density of CD8-, CD163-, and PD-1–positive cells was similar in viral infected and infected patients ($P > 0.05$ for all comparisons). Similarly, a significant difference in the expression of LAG-3 or PD-L1 in virally infected and uninfected patients was not identified (see Fig. 3). In addition, there was no association among presence of underlying cirrhosis, pathologic stage, high tumor grade, vascular invasion, or alpha-fetoprotein (AFP) level before surgery and the density of CD8, CD163, PD-1, PD-L1, and LAG-3 expression in tumor ($P > 0.05$ for all comparison). The

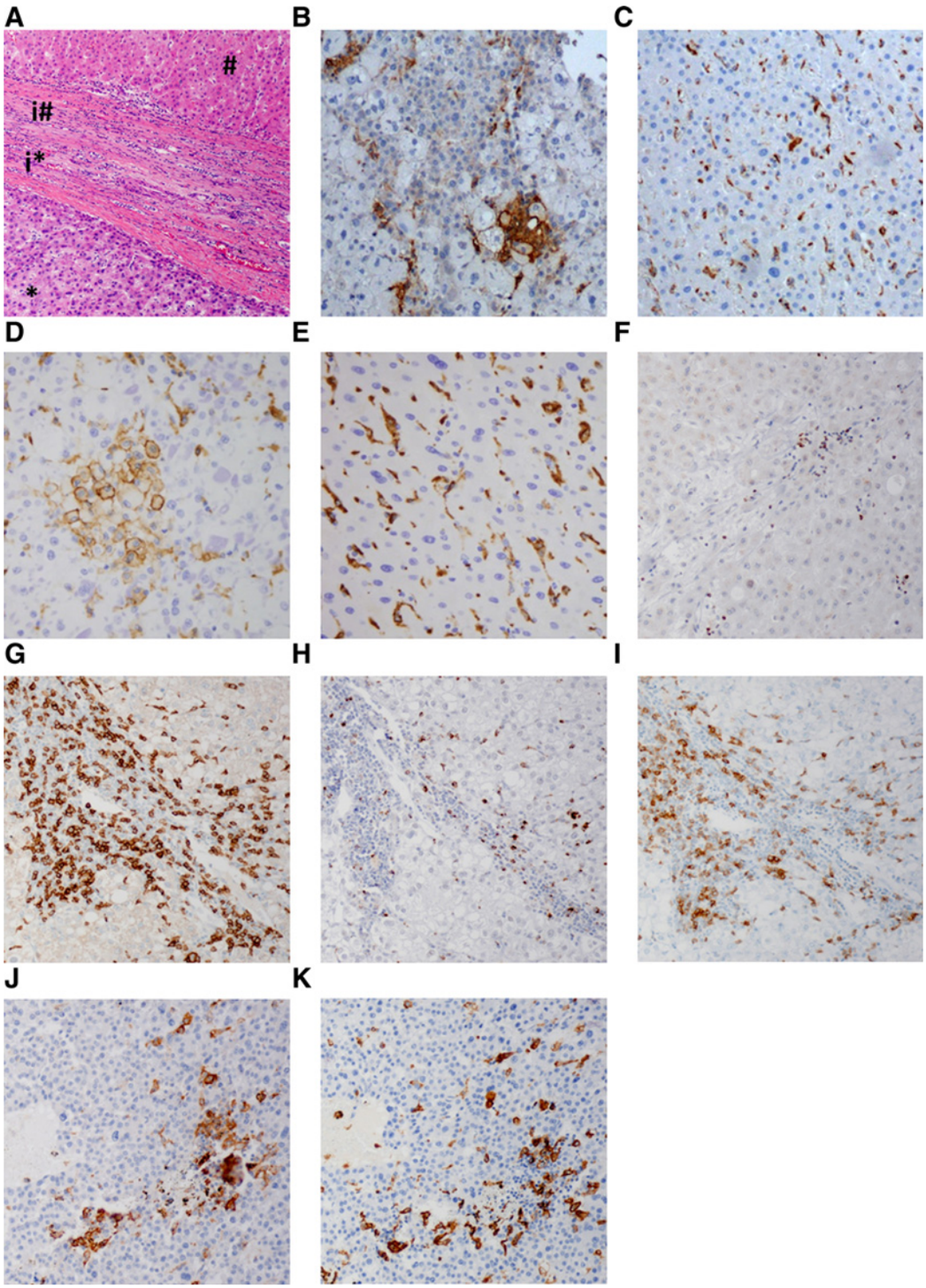

Figure 1.

A, H&E staining of the tumor (*), interface tumor side (i*), interface background side (i#), with background cirrhotic liver (#; magnification, ×10). **B,** Higher-power view of the PD-L1 stain in tumor showing positive cell clusters (magnification, ×40). **C,** Higher-power view of the PD-L1 stain in background liver showing canalicular staining pattern (magnification, ×40). **D,** Higher-power view of the CD163 in tumor showing clusters of tumor-infiltrating macrophages (magnification, ×40). **E,** Higher-power view of the CD163 in background liver showing a sinusoidal staining pattern (magnification, ×40). **F,** Higher-power view of LAG3 staining on tumor-infiltrating lymphocytes (magnification, ×20). **G,** CD8 staining of tumor revealing a cluster of lymphocytes (magnification, ×20). **H,** LAG3 staining of the same microscopic field as in **G**. **I,** PD-1 staining of the same microscopic field as in **G**. **J,** PD-L1 staining in tumor showing positive cell clusters (magnification, ×20). **K,** CD163 stain of the same microscopic field as in **J**, showing clusters of staining that colocalize with areas of high PD-L1 staining.

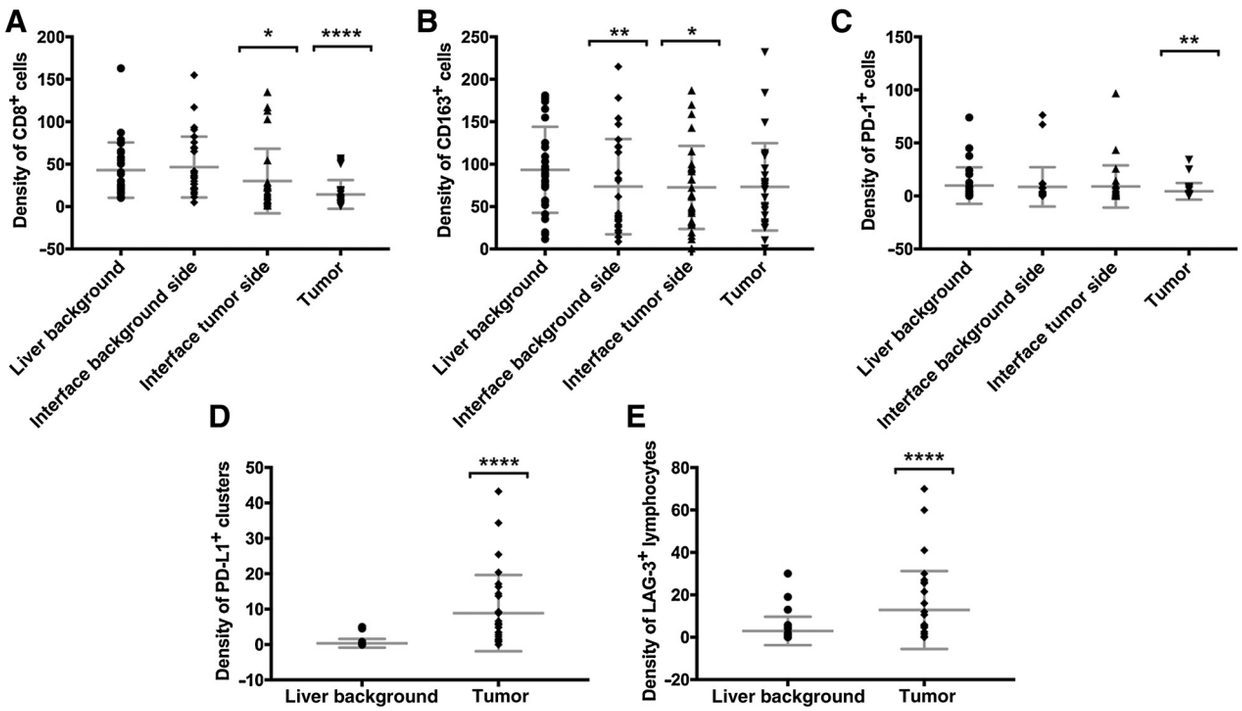

Figure 2.

Density of CD8-, CD163-, and PD-1–positive cells (cells/mm^2) in liver background as compared with tumor interface background side, tumor interface tumor side, and tumor (**A–C**). Density of PD-L1–positive clusters per mm^2 and the percentage of tumor-infiltrating lymphocytes staining positive for LAG-3 in liver background and tumor (**D** and **E**). Density (*y*-axis) in each figure is described per mm^2 of tissue analyzed. Error bars indicate mean and standard deviation; for each comparison with liver background, *, $P < 0.05$; **, $P < 0.01$; ***, $P < 0.001$; ****, $P < 0.0001$.

relationship between tumor pathologic stage and expression of LAG-3 and PD-L1 is displayed in Fig. 4.

Discussion

In this study, we describe the density of CD8, CD163, PD-1, PD-L1, and LAG-3 expression in HCC. Consistent with prior reports, we demonstrate that PD-L1 expression is increased on HCC cells relative to liver background. We also demonstrate that there is a relative decrease in the density of CD8-positive lymphocytes and PD-1–positive cells infiltrating HCC cells, and a relative decrease in the density of CD163-positive cells within the tumor interface, relative to the liver background. Furthermore, we demonstrated for the first time that LAG-3 expression is increased in tumor-infiltrating lymphocytes relative to liver background in patients with HCC. This is also the first study to compare the tumor microenvironment of HCCs derived from a virally infected group versus the uninfected group.

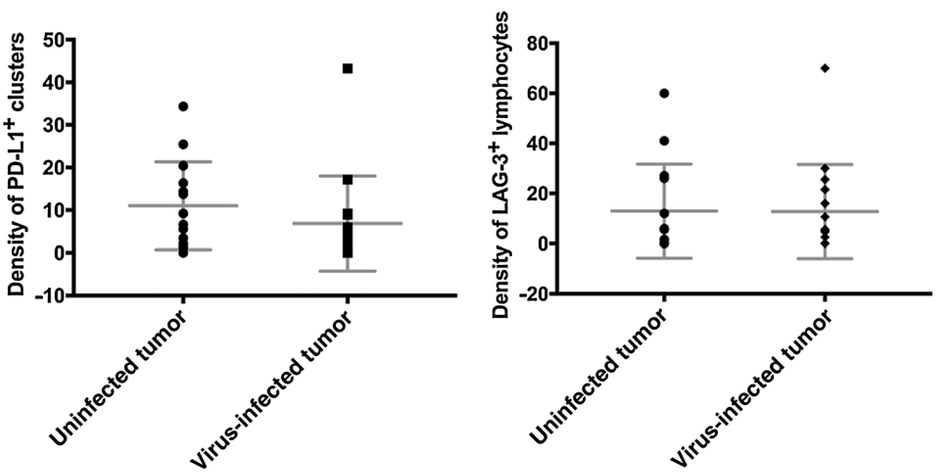

Figure 3.

Density of PD-L1–positive clusters (left) and the percentage of tumor-infiltrating lymphocytes staining positive for LAG-3 (right) were similar in tumor from viral uninfected and infected patients.

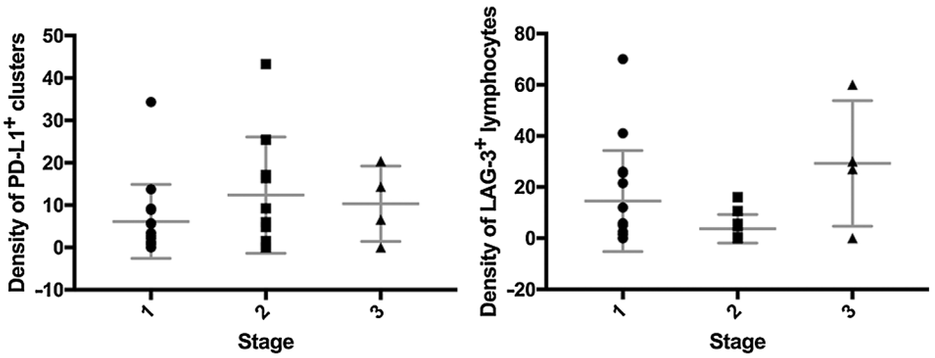

Figure 4.
Density of PD-L1–positive clusters (left) and the percentage of tumor-infiltrating lymphocytes staining positive for LAG-3 (right) were not associated with pathologic tumor stage.

This work has several potential implications. First, the confirmation of elevated PD-L1 expression in HCC tumors supports the continued development of immune checkpoint inhibitors targeting the PD-1/PD-L1 pathway in HCC. Second, the reported expression levels of CD8 and PD-L1 in HCC may serve as a benchmark to evaluate novel therapies that seek to prime tumors for immune checkpoint inhibitory therapy by inducing tumor infiltrating lymphocytes and augmenting PD-L1 expression in HCC. Third, our results newly identify LAG-3 as a potential target for cancer immunotherapy in HCC.

LAG-3 is an immune checkpoint molecule that negatively regulates T-cell function (14). The expression of LAG-3 in some HCCs indicate a likely role for LAG-3 in the suppression of antitumor immunity in HCC and provide a basis for investigating combinatorial checkpoint blockade with a LAG-3 and PD-L1 inhibitor in HCC. LAG-3 inhibition has been proposed to work synergistically with PD-1 inhibition to increase antitumor immunity, and several mAbs that inhibit LAG-3 are now in early human clinical trials (19, 20). The majority of HCC cases with positive PD-L1 staining examined in this study also had increased LAG-3 expression in tumor-infiltrating lymphocytes, suggesting that the LAG-3 immune checkpoint may limit the efficacy of single-agent PD-1 checkpoint blockade in HCC. Furthermore, we identified multiple cases in which there was a discordance between PD-L1 and LAG-3 staining, in which only one of the two immune checkpoints was upregulated. Although it is unknown whether PD-L1 or LAG-3 expression is a predictive biomarker of response to checkpoint inhibitors targeting these pathways in HCC, it is possible that some patients with HCC may benefit from LAG-3 inhibition rather than PD-1 pathway inhibition.

We did not identify any relationship between patient features, tumor histology or stage, or viral status, and expression of any IHC marker in the tumor microenvironment. This could explain the similar response rates observed in clinical trials of immune checkpoint inhibitors between virally infected and uninfected individuals (3–5). However, larger sample sizes are needed to determine more conclusively that expression of these tumor markers is independent of viral status and other clinicopathologic features. Notable strengths of this study include the use of clinicopathologically diverse cases and the use of semiquantitative image analyses or manual scoring of IHC by two pathologists. Relative weaknesses include the modest size of the study cohort. Although the clinical features of the cases were withheld from the pathologists while they performing the manual IHC scoring, the pathologists may have been able to ascertain clinical phenotypes from the pathologic features of the cases. In addition, because this study was exploratory in nature, we did not correct our statistical analysis for the use of multiple comparisons. In conclusion, we have characterized the immune microenvironment in HCC and identified LAG-3 as a potential target for HCC immunotherapy.

Disclosure of Potential Conflicts of Interest

E.M. Jaffee reports receiving commercial research grants from Aduro Biotech, Amgen, and Bristol-Myers Squibb, and is a consultant/advisory board member for Genocea Oncology, Incyte Corp, and Parker Institute. J. Taube reports receiving commercial research grants from Bristol-Myers Squibb, and is a consultant/advisory board member for Astra Zeneca, Bristol-Myers Squibb, and Merck. No potential conflicts of interest were disclosed by the other authors.

Authors' Contributions

Conception and design: D. Xing, T.M. Pawlik, E.M. Jaffee, R.A. Anders
Development of methodology: M. Yarchoan, D. Xing, H. Xu, R.B. Sharma, T.M. Pawlik, Q. Zhu, J.M. Taube, R.A. Anders
Acquisition of data (provided animals, acquired and managed patients, provided facilities, etc.): M. Yarchoan, D. Xing, T.M. Pawlik, E.M. Jaffee, R.A. Anders
Analysis and interpretation of data (e.g., statistical analysis, biostatistics, computational analysis): M. Yarchoan, D. Xing, L. Luan, A. Popovic, T.M. Pawlik, Q. Zhu, E.M. Jaffee, R.A. Anders
Writing, review, and/or revision of the manuscript: M. Yarchoan, D. Xing, R.B. Sharma, A. Popovic, T.M. Pawlik, A.K. Kim, E.M. Jaffee, J.M. Taube, R.A. Anders
Administrative, technical, or material support (i.e., reporting or organizing data, constructing databases): J.M. Taube, R.A. Anders
Study supervision: E.M. Jaffee
Other (developed and performed related IHC staining): H. Xu

Grant Support

This work was partially supported by a NIH grant (T32 CA009071; to M. Yarchoan).

The costs of publication of this article were defrayed in part by the payment of page charges. This article must therefore be hereby marked *advertisement* in accordance with 18 U.S.C. Section 1734 solely to indicate this fact.

Received April 20, 2017; revised July 12, 2017; accepted September 11, 2017; published OnlineFirst September 19, 2017.

References

1. Park J-W, Chen M, Colombo M, Roberts LR, Schwartz M, Chen P-J, et al. Global patterns of hepatocellular carcinoma management from diagnosis to death: the BRIDGE Study. Liver Int 2015;35:2155–66.
2. El-Serag HB. Hepatocellular carcinoma. N Engl J Med 2011;365:1118–27.
3. El-Khoueiry AB, Sangro B, Yau T, Crocenzi TS, Kudo M, Hsu C, et al. Nivolumab in patients with advanced hepatocellular carcinoma

(CheckMate 040): an open-label, non-comparative, phase 1/2 dose escalation and expansion trial. Lancet 2017;389:2492–502.
4. Zhu A, Knox J, Kudo M, Chan S, Finn R, Siegel A, et al. Pembrolizumab in patients with previously treated advanced hepatocellular carcinoma: phase 2 KEYNOTE-224 study. Ann Oncol 2016;27.
5. Wörns MA, Galle PR, Amaddeo G. Immune oncology in hepatocellular carcinoma-hype and hope. Lancet 2017;64:2038–46.
6. Sangro B, Gomez-Martin C, de la Mata M, Iñarrairaegui M, Garralda E, Barrera P, et al. A clinical trial of CTLA-4 blockade with tremelimumab in patients with hepatocellular carcinoma and chronic hepatitis C. J Hepatol 2013;59:81–8.
7. Wu K, Kryczek I, Chen L, Zou W, Welling TH. Kupffer cell suppression of CD8+ T cells in human hepatocellular carcinoma is mediated by B7-H1/programmed death-1 interactions. Cancer Res 2009;69:8067–75.
8. Shi F, Shi M, Zeng Z, Qi R-Z, Liu Z-W, Zhang J-Y, et al. PD-1 and PD-L1 upregulation promotes $CD8^+$ T-cell apoptosis and postoperative recurrence in hepatocellular carcinoma patients. Int J Cancer 2011;128:887–96.
9. Gao Q, Wang X-Y, Qiu S-J, Yamato I, Sho M, Nakajima Y, et al. Overexpression of PD-L1 significantly associates with tumor aggressiveness and postoperative recurrence in human hepatocellular carcinoma. Clin Cancer Res 2009;15:971–9.
10. Calderaro J, Rousseau B, Amaddeo G, Mercey M, Charpy C, Costentin C, et al. Programmed death ligand 1 expression in hepatocellular carcinoma: relationship with clinical and pathological features. Hepatology 2016;64:2038–46
11. Waidmann O, Köberle V, Bettinger D, Trojan J, Zeuzem S, Schultheiß M, et al. Diagnostic and prognostic significance of cell death and macrophage activation markers in patients with hepatocellular carcinoma. J Hepatol 2013;59:769–79.
12. Kazankov K, Rode A, Simonsen K, Villadsen GE, Nicoll A, Møller HJ, et al. Macrophage activation marker soluble CD163 may predict disease progression in hepatocellular carcinoma. Scand J Clin Lab Invest 2016;76:64–73.
13. Kong L-Q, Zhu X-D, Xu H-X, Zhang J-B, Lu L, Wang W-Q, et al. The clinical significance of the CD163+ and CD68+ macrophages in patients with hepatocellular carcinoma. In: Villa E, editor. PLoS ONE 2013;8:e59771.
14. Topalian SL, Drake CG, Pardoll DM. Immune checkpoint blockade: a common denominator approach to cancer therapy. Cancer Cell 2015;27:450–61.
15. Yanik EL, Kaunitz GJ, Cottrell TR, Succaria F, McMiller TL, Ascierto ML, et al. Association of HIV status with local immune response to anal squamous cell carcinoma. JAMA Oncol 2017;21287:1–5.
16. Lipson EJ, Lilo MT, Ogurtsova A, Esandrio J, Xu H, Brothers P, et al. Basal cell carcinoma: PD-L1/PD-1 checkpoint expression and tumor regression after PD-1 blockade. J Immunother Cancer 2017;5:23.
17. Le D, Uram J, Wang H, Kemberling H, Eyring A, Bartlett B, et al. PD-1 blockade in mismatch repair deficient non-colorectal gastrointestinal cancers. J Clin Oncol 2016;34:195.
18. Cuka N, Hempel HA, Sfanos KS, De MarzoAM, Cornish TC. PIP: an open source framework for multithreaded image analysis of whole slide images. Lab Investig 2014;94:398A.
19. Woo S-R, Turnis ME, Goldberg MV, Bankoti J, Selby M, Nirschl CJ, et al. Immune inhibitory molecules LAG-3 and PD-1 synergistically regulate T-cell function to promote tumoral immune escape. Cancer Res 2012;72:917–27.
20. Matsuzaki J, Gnjatic S, Mhawech-Fauceglia P, Beck A, Miller A, Tsuji T, et al. Tumor-infiltrating NY-ESO-1-specific $CD8^+$ T cells are negatively regulated by LAG-3 and PD-1 in human ovarian cancer. Proc Natl Acad Sci U S A 2010;107:7875–80.